Multilayering of Calcium Aerosol-OT at the Mica/Water Interface Studied with Neutron Reflection – Formation of a Condensed Lamellar Phase at CMC

[1]L. R. Griffin, [1]K. L. Browning, [1]S.Y. Lee, [2]M. W. A. Skoda, [2]S. Rogers and [1]S. M. Clarke,*

[1] BP Institute and Department of Chemistry, University of Cambridge, Cambridge, CB3 0EZ

[2] ISIS Facility, Science and Technology Facilities Council, Rutherford Appleton Laboratory, Didcot, Oxfordshire, UK, OX11 0QX

Abstract

Using specular neutron reflection, the adsorption of sodium and calcium salts of the surfactant bis(2-ethylhexyl) sulfosuccinate (Aerosol-OT or AOT) has been studied at the mica/water interface at concentrations between 0.1 and 2 CMC. The pH dependence of the adsorption was also probed. No evidence of the adsorption of Na(AOT) was found even at the critical micelle concentration (CMC) whilst the calcium salt was found to adsorb significantly at concentrations of 0.5 CMC and above. This interesting and somewhat

unexpected finding demonstrates that counter-ion identity may be used to tune the adsorption of anionic surfactants on anionic surfaces. At the CMC, three condensed bilayers of $Ca(AOT)_2$ were adsorbed at pH 7 and 9 and four bilayers adsorbed at pH 4. Multilayering at the CMC of $Ca(AOT)_2$ on the mica surface is an unusual feature of this surfactant/surface combination. Only single bilayer adsorption has been observed at other surfaces at the CMC. We suggest this arises from the high charge density of mica which must provide an excellent template for the surfactant.

Key words

Aerosol-OT; Mica; NaAOT; $Ca(AOT)_2$; multilayers; surfactant; adsorption; neutron reflection

Introduction

Surfactant adsorption at interfaces lies at the heart of numerous academic and commercial problems. These systems exhibit a diverse range of behaviors at interfaces dependent on surface identity, surfactant identity, temperature and concentration.

The multilayer structures of a number of adsorbed surfactants at the air/water interface have been recently surveyed in a review by Thomas and Penfold, often based on neutron reflection data[1]. They report a variety of behaviors conveniently characterized by the layer spacing and the number of layers at the surface, relative to the bulk solution behavior.

As described in the Thomas and Penfold reference, they adopt the S_n notation which corresponds to n distinct molecular layers at the surface separated from one another by

solvent. Here, n is a small number such that it can be determined within the instrumental resolution of the experimental measurement (essentially line broadening above that of the experimental resolution). In contrast, S_N (capitalized N) is applied when N is somewhat larger and cannot be experimentally determined.

This notation has been used to describe layering at the mica/water interface throughout this work, although we include a prime S'_n to reflect the fact that all n layers in our case are bilayers adsorbed at a hydrophilic surface, contrasting with the monolayer and additional bilayers evident in the adsorption at the 'hydrophobic' air/water interface of the Thomas and Penfold work.

The following terms from the review by Thomas and Penfold used to describe an adsorbed surfactant lamellar phase have also been adopted in this article: $L_\alpha(n)$normal concentrated lamellar phase where the surfactant layers have very little solvent between them, $L_\alpha(sf)$ space filling phase (lamellar d-spacing changes to fill the volume available), $L_\alpha(c)$ for a concentrated phase that exists in dilute solution (layer repeat spacing ~30 - 60 Å) and $L_\alpha(sw)$ the swollen phase with considerable solvent between the surfactant bilayers, but with a fixed period, (the interlamellar distances are of order 100 - 200 Å or greater).

In this work, we report on the adsorption behavior of the surfactant Aerosol OT, and the changes in behavior with differing counter-ions. Aerosol-OT (sodium bis(2-ethylhexyl)sulfosuccinate, NaAOT) is a branched anionic dichain surfactant. The CMC of NaAOT at 25 °C in pure water is 2.5 mM, with the onset of the lamellar phase ($L_1 + L_\alpha$) occurring at approximately 50 mM[2–4]. Li *et al.* measured the bulk lamellar phase of NaAOT using small angle neutron scattering and report that the lamellar spacing is highly sensitive to concentration and temperature. The lamellar phase remains relatively swollen with d-spacings between 325 Å and 175 Å, much larger than the bilayer thickness (an $L_\alpha(sw)$ phase).

Different salts of AOT have been prepared by exchanging the sodium with an excess of a different ion using the method of Eastoe *et al.*[5]. The CMC of $Ca(AOT)_2$ is reduced relative to NaAOT to 0.5 mM, as is typically for calcium surfactants[6,7]. The divalent counter ion also lowers the concentration for the onset of the bulk lamellar phase ($L_1 + L_\alpha$) to 1.1 mM[8]. We are not aware of any existing work which comprehensively reports the lamellar phase spacing for $Ca(AOT)_2$.

The sodium salt of the AOT surfactant has been widely studied at both the air/liquid and solid/liquid interface using neutron reflection both above and below the CMC[2,6,9–12]. Fewer measurements of $Ca(AOT)_2$ at solid/liquid interfaces have been made[6,11]. Reported adsorption characteristics of NaAOT and $Ca(AOT)_2$ at these various interfaces are now briefly discussed.

*Adsorption of AOT **c**lose to the CMC:*

At the air/water interface NaAOT is adsorbed as a monolayer with increasing surface coverage over the concentration range CMC/300 to CMC[2]. The complete monolayer was 18 Å thick with an area per molecule (APM) 78 ± 3 $Å^2$ [2]. A monolayer is formed because the air interface is considered more hydrophobic than (hydrophilic) water. Fragneto *et al.* made similar observations on hydrophobic silicon (silicon with a grafted layer of octadecyltrichlorosilane), where the adsorption of AOT was observed over the concentration range CMC/100 to CMC. At the CMC, the adsorbate was a monolayer with APM of 80 ± 5 $Å^2$ and thickness 15 ± 2 Å[9].

Adsorption of NaAOT on alumina between 0.2 to 7.4 mM (0.1 - 3.0 CMC) was measured by Hellsing and Rennie, where a bilayer of constant thickness, 33 ± 2 Å, was adsorbed with an APM at the CMC of 57 ± 6 $Å^2$ and 12 water molecules per AOT headgroup[10]. Adding

electrolyte to a solution below the CMC increased the observed adsorption and the effect of different monovalent salts was very similar. The effect of changing the pH and added electrolyte was equivalent and was interpreted as an ionic strength effect. The pH invariance of the adsorption suggests that hydrophobic interactions between surfactant molecules, as opposed to electrostatic attraction to the surface, dominates the adsorption of AOT on alumina[10].

Stocker *et al.* compared the adsorption of the sodium and calcium AOT salts at the cationic calcite/water interface. At the CMC, a 35 ± 3 Å bilayer was observed for both NaAOT and $Ca(AOT)_2$ with areas of 86 ± 14 $Å^2$ and 61 ± 14 $Å^2$ per AOT moiety respectively[11].

Interesting behavior was observed on hydrophilic silica[6]. Perhaps unsurprisingly, no adsorption of the sodium salt of this anionic surfactant on the anionic surface was observed at the CMC. In contrast, the calcium salt was found to adsorb at concentrations above 0.5 CMC. A cation bridging mechanism was suggested to explain the adsorption; a mechanism that would only be appropriate in the presence of multivalent ions (such as divalent calcium) and not monovalent ions (such as sodium). At the CMC, a bilayer of thickness 35 ± 7 Å at pH 7 and 38 ± 7 Å at pH 9, with evidence of increased adsorption at pH 9, was measured. The increased adsorption at higher pH was suggested to result from a higher density of negative $Si\text{-}O^-$ surface groups, providing more adsorption sites. The measured APM was 70 ± 5 $Å^2$ at pH 7 and 74 ± 5 $Å^2$ at pH 9. No adsorption was measured at pH 4 where the density of $Si\text{-}O^-$ groups is expected to be small.

Using the nomenclature of Penfold and Thomas, the observations at all the interfaces discussed above can be described as S_1' surface structures.

Adsorption of the AOT Lamellar Phase:

Adsorption of the lamellar phase of NaAOT has been studied at both the air/water and solid/liquid interfaces where generally only slight perturbations of the bulk repeat spacings

are observed in the adsorbed layer. At 25°C for surfactant concentrations between 2 and 10% w/w, lamellar repeat spacings at the air/water, calcite/water, sapphire/water and silica/water interfaces are reported in the range 170 - 220 Å[11–15]. These structures can be classified as $L_\alpha(sw)$ phases, where the substrate provides a template for reorientation of the bulk lamellar phase. There is long range order in the direction normal to the surface, albeit with a slightly reduced repeat spacing in the adsorbed lamellar phase.

In this paper we use neutron reflection to study NaAOT and $Ca(AOT)_2$ at the mica/water interface. Whilst mica has long been an important material in surface studies being widely used in atomic force microscopy (AFM) and surface force apparatus (SFA) experiments, reflection methods for studying the surface have only recently been innovated[16,17].

X-Ray Reflection (XRR) was achieved by bending a thin sheet of mica along a cylinder to achieve the required flatness along the axis of the cylinder. Several polymer and surfactant systems have been studied in this elegant fashion by Briscoe *et al*[17–19].

An alternative method to study the mica interface using neutron reflection was developed by Browning *et al*. and has been successfully applied to several surfactant sytems[16,20,21].

Mica is a highly absorbing material to neutrons and the presence of defects in this naturally occurring material also contribute significantly to attenuation of the neutron beam, resulting in difficulty with transmission through the mica.

Browning *et al.* showed that these difficulties can be avoided by supporting a thin film of mica on a silicon wafer. The adhesion of this thin film to a neutron reflection grade silicon wafer circumvents flatness and transmission problems enabling data with molecular precision to be recorded from the mica/liquid interface[16,20,21]. Some care in data interpretation is required particularly the treatment of beam attenuation and incoherent combination of reflected signals from interfaces separated by larger distances[16,20,21].

Experimental

Substrate preparation

The preparation of mica substrates for neutron reflection is described in detailed elsewhere and is only outlined here[16]. Silicon wafers (50 mm × 100 mm × 10mm, single side polished, N-type, (111) face from Crystran, UK) were soaked in nitric acid for four hours, rinsed ten times in Millipore water (18.2 MΩ cm^{-1}) and soaked overnight. Remaining organic contaminants were removed by UV Ozone cleaning (Bioforce Nano) for 10 minutes. 1 mL of Loctite 3301 UV curable glue was passed through a Millipore filter (0.22 μm) on to the clean silicon wafer and spun at 5000 RPM for 5 minutes. Meanwhile, adhesive tape was stuck down uniformly to both sides of a 50 mm × 100 mm × 25 μm muscovite mica sheet (Attwater and Sons, UK) by passing a stiff card across the surface. A new clean mica surface was created by cleaving the mica between the basal planes by peeling back the adhesive tape. A few drops of water were added to the new surface to lower the energy of surface formation and aid smooth cleavage. The new mica surface was allowed to dry and then stuck down to the glue coated silicon wafer. A stiff card was swiped across the surface to eliminate air bubbles between the mica and glue layers. The mica coated silicon crystal was placed against a Pyrex block of neutron grade flatness and clamped between two Perspex plates through which the glue was cured for 1 hour using a UV lamp ($\lambda > 385$ nm). The surface used for reflection was revealed by a further peeling back of the silicon bound mica by adhesive tape, once again dropping water into the newly created surface to aid cleavage. Any remaining organic contaminants were removed by UV ozone cleaning before the silicon block and mica were clamped to a water filled PTFE trough held in place by metal plates to create the mica/water interface.

Chemicals

Sodium bis(2-ethylhexyl) sulfosuccinate (≥ 99.0% purity), NaAOT, was purchased from Sigma-Aldrich and used to prepare Calcium AOT samples by liquid/liquid ion exchange, using the procedure of Eastoe *et al.*[22]. NaAOT was also purified as described by Li *et al.* and dried in a vaccum oven[2].

Surfactant purity was checked using elemental analysis, ICP, ^{1}H and ^{13}C NMR. This analysis was performed on a separate batch of sample prepared in an identical fashion to those run at ISIS. ICP measurements showed that the quality of calcium for sodium exchange was > 99 %. The NMR indicated the correct resonances expected, with an additional single peak at 3.6 to 3.8 ppm which we attribute to water impurity.

Stock solutions of $Ca(AOT)_2$ were prepared at a concentration on 2 CMC and diluted to the required concentrations for experiments. A small amount of the $Ca(AOT)_2$ stock solution did not dissolve, hence the concentrations for the neutron experiments are possibly slightly lower than stated because the stock solution was close to the solubility limit of the sample.

The D_2O used in this study was supplied by the ISIS neutron facility (Sigma 99.9 atom % D) and all H_2O was from an ultrapure supply (Millipore 18.2 MΩ cm^{-1}). The pH of samples was changed by the addition of NaOH (Sigma ACS reagent, ≥ 97.0%), DCl (Sigma 99 atom % D) or HCl (ACS reagent, 37%).

Freshly prepared mica substrates were sealed against Teflon troughs as outlined above. The Teflon troughs were cleaned by soaking in concentrated nitric acid (Sigma ACS reagent, 70%) for four hours, rinsing ten times in ultrapure water and allowing to soak in water overnight.

All glassware was cleaned using nitric acid as described above. Plastic bottles, spatulas and tubing were cleaned using Decon 90 and rinsed copiously in ultrapure water. The HPLC

pump (L7100 HPLC pump, Merck, Hitachi) and lines were cleaned by passing ethanol through all the components followed by pumping through ultrapure water for 20 minutes.

The cells were filled by introducing liquid to the bottom of the cell using an HPLC pump at a flow rate of 5 mL min^{-1}, whilst gently rocking until no air bubbles could be seen in the liquid out line. All solution changes were carried out in-situ using the pump system by passing 20 mL (~10 cell volumes) of solution through the cell at 2 mL min^{-1}. The Teflon troughs, specially designed for their flow properties, are known to exchange thoroughly using this procedure.

Different neutron scattering contrast solutions were prepared by pumping D_2O and H_2O in the required volume ratios using the HPLC pump. All water described as contrast matched to silicon (CMSi) was prepared by pumping 38% D_2O and 62% H_2O by volume into the sample cell resulting in a scattering length density of 2.07×10^{-6} $Å^{-2}$.

Neutron reflection measurements

Neutron reflection measurements were made using the INTER reflectometer at the STFC Rutherford Appleton Laboratory (Didcot, UK)[23,24]. All measurements were made in time of flight mode using the wavelength range 1 to 15 Å and three incident angles 0.4°, 1.5° and 3.2° to cover the full range of momentum transfer to the surface, Q, of 0.006 to 0.3 $Å^{-1}$. A series of collimating slits prior to the sample were used to maintain a constant beam footprint of 35 × 75 mm on the substrate across all three angles of incidences. These slit settings resulted in an instrumental resolution $\Delta Q/Q$ of 3%. Data were collected using a single detector and normalised against a transmission run recorded through the silicon wafer.

SANS measurements

SANS measurements were made using the SANS2D instrument at the STFC Rutherford Appleton Laboratory (Didcot, UK)[23,25]. This is a fixed geometry time of flight instrument utilizing neutron wavelengths between 1.75 and 16.5 Å. An instrument setup of L1 = L2= 4 m with the rear 1 m^2 detector offset vertically 75 mm and sideways 100 mm and beam diameter of 8 mm was used to cover the Q range 0.004 to 0.7 $Å^{-1}$ for the reported measurements. Samples were prepared in deuterated solvents to provide sufficient contrast and were placed in 2 mm path length quartz cuvettes and measured for 1 hour. Raw scattering data was corrected for detector efficiencies, sample transmission and background scattering and converted to scattering cross section data using instrument specific software[26]. These data were placed on an absolute scale (cm^{-1}) using the scattering from a standard sample (a solid blend of hydrogenous and perdeuterated polystyrene) in accordance with established procedures[27].

Data fitting

Neutron reflectivity data was analysed using a fitting package, I-CALC, developed in house. As described in our previous papers, mica substrates for neutron reflection contain both thick and thin layers[16,20].

Thin layers, usually encountered in neutron reflectivity, are those whose thicknesses are smaller than the coherence length of the neutron radiation. Here the amplitudes of reflected beams should be added as described by Heavens[28]. The reflectivity arising from a series of thin layers is commonly analysed using the Abeles matrix formulism[28]. In this work, the sample has thin layers of the native oxide on the silicon and the adsorbed surfactant. Thick layers, such as the mica and glue layers in our samples, are those whose thickness is greater than the coherence length of the neutrons radiation. Here there is a loss of coherence of the

radiation as it passes across the sample from one interface to another. In this case, there is no interference/phase term but instead the reflected intensities of emergent beams are damped by an attenuation term[16,29]. The attenuation of the neutron beam as a function of wavelength by mica and Loctite® 3301 glue has been experimentally measured as reported in previous publications[21]. The Supporting Information has further details of this thick layer calculation. The coefficients for the attenuation correction for the glue layer were mis-labelled in a previous publication, despite being correctly employed in calculations. The correct form of the attenuation cross section and the coefficients are as given in Eq 1.

$$N\sigma_{tot,glue}(\lambda) = \alpha_{glue} + \beta_{glue}\lambda + \gamma_{glue}\lambda^2 + \delta_{glue}\lambda^3 \quad \textbf{Eq 1}$$

$$\alpha_{glue} = -(31 \pm 4) \times 10^{-9}\text{Å}^{-4}$$

$$\beta_{glue} = -(5.7 \pm 0.9) \times 10^{-9}\text{Å}^{-3}$$

$$\gamma_{glue} = (0.19 \pm 0.07) \times 10^{-9}\text{Å}^{-2}$$

$$\delta_{glue} = -(0.004 \pm 0.002) \times 10^{-9}\text{Å}^{-1}$$

The I-CALC reflectivity program calculates the reflectivity profile according to a combination of these two ('thick' and 'thin') approaches as reported previously[16,20].

Results

Adsorption of NaAOT and $Ca(AOT)_2$ at pH 7

Material	SLD/ × 10^{-6} Å^{-2}
Silicon	2.07
Silicon Oxide	3.49
Glue	0.88[a]
Mica	3.79
D_2O	6.35
H_2O	-0.56
Contrast matched water to silicon (CMSi)	2.07

Table 1: Fitted scattering length densities of materials used during this study. [a]Calculated from chemical formula $C_{41}H_{65}NO_{15}$ determined by elemental analysis of the glue studied and the cured glue density, 1.16 g cm^{-3} (from Loctite 3301 Technical Data Sheet)

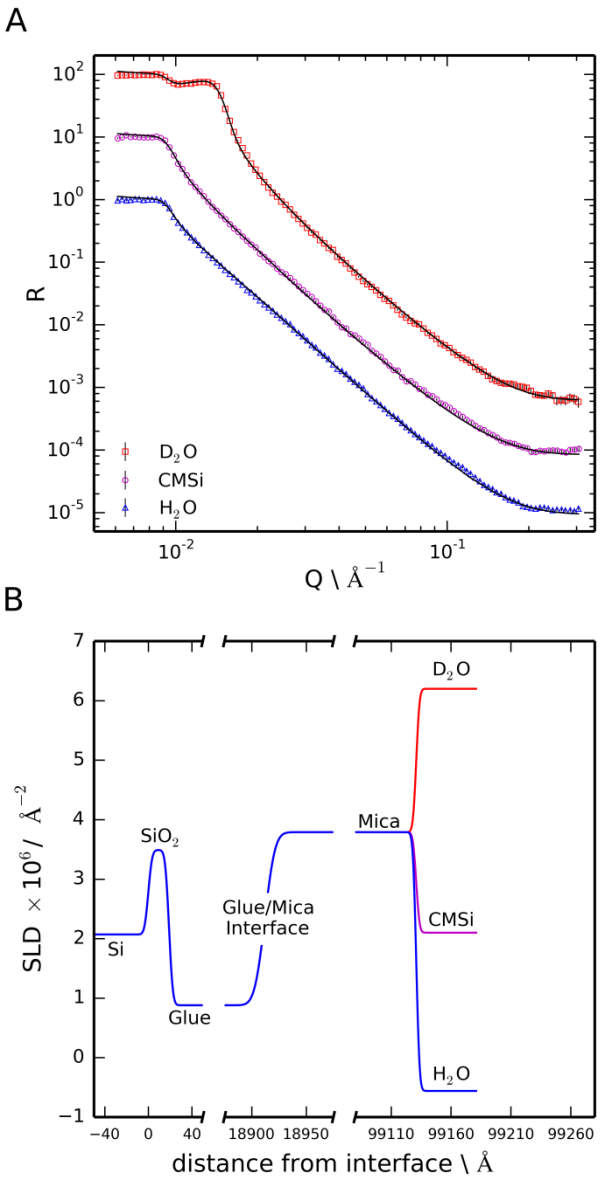

Figure 1: *A)* Observed (points) and calculated reflectivity profiles (lines) for the bare surface in D_2O (squares), CMSi water (circles) and H_2O (triangles). Fitted lines are calculated for the bare surface according to a three layer model using the parameters given in Table 2. D_2O and CMSi data sets are offset for clarity. *B)* SLD profiles extracted from fits. The horizontal axis is split for clarity at interfaces of interest. Error bars have been included in the figure.

Layer	Thickness	Roughness/ Å
Silicon Substrate	-	3 ± 2 Å
Silicon Oxide	19 ± 2 Å	3 ± 2 Å
Glue	1.9 ± 0.5 µm	7± 2 Å
Mica	8.0 ± 2 µm	2 ± 2 Å

Table 2: Parameters used for fitting of the bare surface reflectivity profiles for the pH 7 crystal.

Neutron reflectivity profiles from the bare mica/water interface were recorded in three contrasts (D_2O, CMSi, H_2O) of water. The structure of the interface is unchanged on changing the water contrast but changing the contrast provides three independent data that allow us to determine the surface structure more uniquely. The three data sets must all fit the same physical structure, even though the scattering power of the water is changing. Here we have assumed that the chemical nature of D_2O and H_2O is identical as this is determined by the electronic properties of the molecules and not by the nuclear properties.Data collected are shown in Figure 1. The D_2O contrast shows a characteristic double critical edge feature. The first critical edge present in all three contrasts at $Q = 0.009\ \text{Å}^{-1}$ is due to total reflection from the glue/mica interface. Beyond this Q value, the beam enters the thick mica layer and reflectivity falls away as neutrons are attenuated on their passage through the layer. The attenuation of the beam is dependent on the attenuation cross section, which is wavelength dependent, and the total path length through the layer linked to the angle of the beam through the layer, which is also wavelength dependent. These factors combined result in a reduction in the attenuation as Q increases and so that a recovery of the reflected intensity towards the second critical edge at $Q = 0.014\ \text{Å}^{-1}$ (corresponding to the mica/D_2O interface) is observed.

Beyond the second critical edge, the beam penetrates into the subphase and a broadly Q^{-4} fall in intensity is observed.

The fits to the data have been found using the I-CALC program by co-refining the data for all three contrasts simultaneously, allowing only the scattering length density of the subphase to vary between contrasts. A three layer model of silicon oxide, glue and mica was used to describe the substrate structure. Thickness and roughness parameters in Table 2 and scattering length densities (SLDs) in Table 1 have been used to generate the fits.

The thickness of the glue layer is rather difficult to determine through neutron reflectivity measurements. Beam attenuation on the passage through this thick layer has the effect of reducing the reflected intensity across the whole Q range; an effect which is difficult to disentangle from experimental factors. As a result, the thickness of the glue layer cannot be determined with certainty. The thickness of the mica layer can be estimated from the reduction in intensity between the two critical edges in the D_2O contrast but still can only be determined to the nearest fraction of a micron, unlike the usual angstrom resolution of the NR technique available for thin films where interference effects are central. The thickness of these two layers (mica and glue) is not of primary interest here and the precision of these layer thicknesses does not significantly affect the final adsorbate structure.

Figure S1 in the Supporting Information clearly indicates that there is essentially no change in the reflectivity on exposure of the mica to the sodium salt of the AOT at the CMC. This indicates that there is no significant adsorption of the sodium salt of the AOT on the mica. Similarly Figure S2 indicates that there is very little adsorption of the Calcium AOT salt at concentrations of 0.1 CMC, 0.25 and 0.5 CMC also show very little evidence of adsorption, only a thin hydrated layer which appears at 0.1 CMC.

A much more significant change in the reflectivity, compared the bare surface measurements, was recorded after the mica surface had been exposed to 1 CMC $Ca(AOT)_2$ at

pH 7 (see Figure 2). This data clearly indicates the presence of an adsorbed ordered structure at the mica/water interface in direct contrast to that observed for NaAOT.

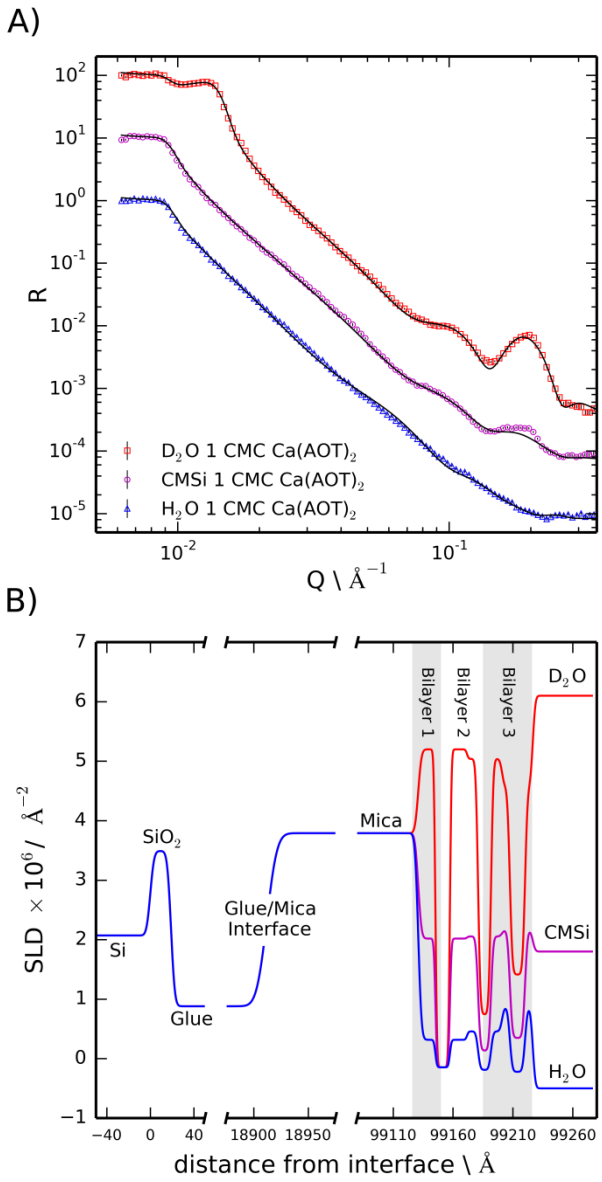

Figure 2: *A)* Observed (points) and calculated reflectivity profiles (lines) for the surface exposed to 1 CMC Ca(AOT)$_2$ at pH 7 in D_2O (squares), CMSi water (circles) and H_2O (triangles). Fits were calculated using a three layer model for the bare surface parameters given in Table 2 and three stacked bilayers using the parameters given in Table 3. Data is offset for clarity. *B)* SLD profiles extracted from fits. The horizontal axis is split for clarity at interfaces of interest. Error bars have been included in the figure.

Layer	APM/ Å^2	Water molecules per head	Water molecules per tail	Roughness/ Å
1	66 ± 3	23 ± 1	0 ± 1	1 ± 1
2	86 ± 4	18 ± 1	4 ± 1	2 ± 1
3	84 ± 4	10± 1	9 ± 1	2 ± 1

Table 3: Parameters used for fitting of the adsorbate structure at 1 CMC at pH 7.

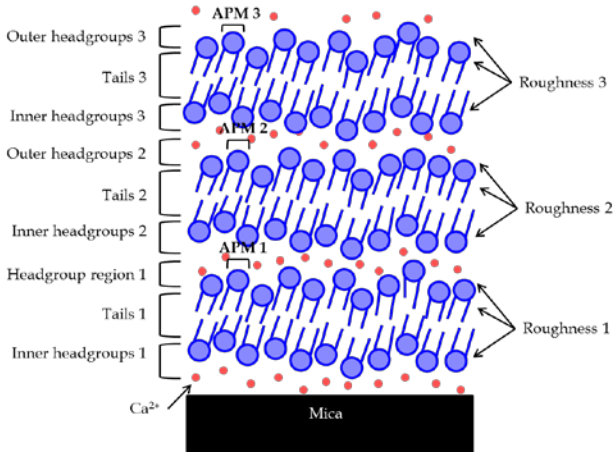

Figure 3: Schematic of three bilayers assembled at the mica/water interface at pH 7 in 1 CMC $Ca(AOT)_2$ and the relevant structural parameters.

A series of plausible adsorbate structures were considered during the fitting procedure -a model consisting of three stacked bilayers without intervening water layers was found to fit the data best, as illustrated in Figure 3.

In this characterization, the model was constrained as much as possible. Each bilayer was assumed to be symmetric in the inner and outer surfactant leaflets and characterized by its own set of parameters. The floating parameters in this model for a single bilayer were the number of water molecules per headgroup, water molecules per tail, area per molecule (APM) and roughness. The same roughness parameter was applied to each of the interfaces

within the bilayer (innerhead/tails, tails/outerheads, outerheads/adjacent layer). These four parameters alongside atomic composition and molecular volumes of the surfactant headgroup and tailgroups are sufficient to define the thickness, SLD and roughness of the three regions of each bilayer (innerheads, hydrocarbon tails, outerheads). This was considered most simple structural model (fewest floating parameters) to adequately describe a bilayer. More complex models were not explored.

Structures consisting of multiple bilayers (2, 3 or 4) were formed by appending extra layers to the stack, each described by its own set of parameters. The D_2O, CMSi and H_2O contrasts were fitted simultaneously to the same structural model only changing the SLD of the subphase.

The bulk density of NaAOT is reported in the range 1.14 to 1.16 g cm^{-3} [9,10,13,30]. This density alongside the molecular weight of NaAOT (444 g mol^{-1}) yields a molecular volume in the bulk crystal in the range 636 to 648 $Å^3$. The molecular volume of $Ca(AOT)_2$ is assumed to be approximately twice the volume of NaAOT since the volume is dominated by the AOT anion. This total volume can be divided between the surfactant headgroup and tailgroups. The volumes and scattering length densities of these regions used during the fitting procedure are given in Table 4, assuming a bulk density of 1.15 g cm^{-3}. Uncertainty in the bulk density and uncertainty in the total volume apportioned the headgroup and tailgroup regions will propagate as uncertainty in the final fitted parameters.

Parameter	½ $Ca(AOT)_2$	Headgroup	Tailgroup
Formula	$Ca_{0.5}C_{20}H_{37}O_7S$	$Ca_{0.5}C_4H_7O_7S$	C_8H_{17}
V_c/ $Å^3$	642	242	200
SLD/ 10^{-6} $Å^{-2}$	0.65	2.59	-0.52

Table 4: Molecular dimensions and scattering length density of $Ca(AOT)_2$. Molecular volumes have been assumed unperturbed from values for NaAOT.

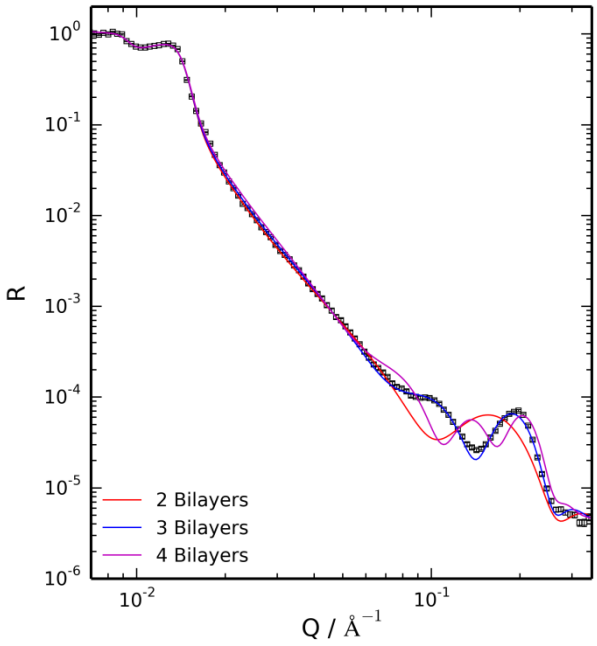

Figure 4: Reflectivity profile recorded for the mica surface exposed to 1 CMC $Ca(AOT)_2$ in D_2O at pH 7 (squares) and fits to the data calculated using models for two, three and four stacked bilayers.

The fits to the reflectivity data in Figure 2 are calculated according the bilayer parameters in Table 3.

For comparison, fits calculated using similar parameters for a two bilayer, three bilayer and four bilayer model are shown in Figure 4. It can be seen that the three layer model captures features in the data significantly better than the other proposal models, strongly suggesting three adsorbed layers is indeed the adsorbed structure.

In this work we have combined the data from reflectivity data in three water contrasts to extract 12 parameters characterising the adsorbate structure. Within this analysis we are confident that the neutron reflection data is able to provide robust information about the number of layers absorbed at the interface. However, precise details on the location of water molecules around the headgroups and tailgroups must be inferred from the scattering length

densities extracted from fringe intensities. This information is, therefore, subject to a greater uncertainty than the number of layers.

We note that it is unusual to find adsorbed multilayers at such a low free surfactant concentration. In keeping with Thomas and Penfold's nomenclature, this structure is described as an S_3' adsorbed concentrated lamellar phase, $L_\alpha(c)$.

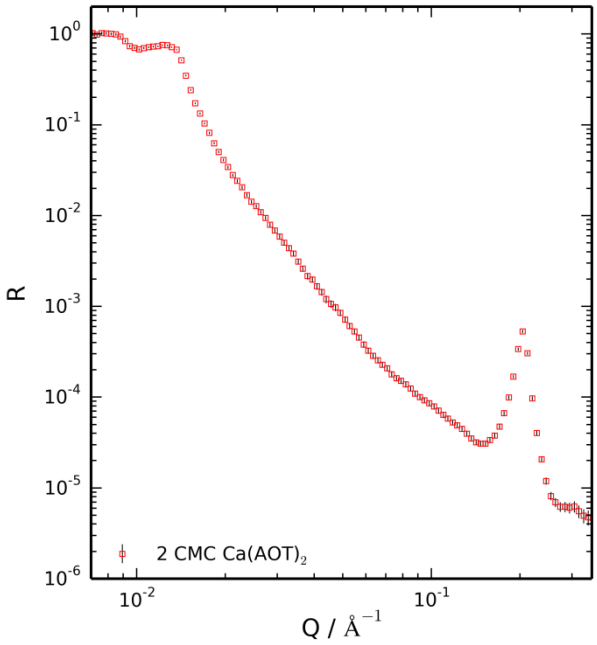

Figure 5: Reflectivity profile collected at the mica/water interface after exposure to $Ca(AOT)_2$ with concentration of 2 CMC at pH 7.

When exposed to $Ca(AOT)_2$ at 2 CMC, the reflectivity profile changed again, losing the broad features seen at 1 CMC. Instead, a single sharp peak is observed at Q = 0.20 Å^{-1} which was interpreted as a Bragg peak from a much larger number of bilayers at the surface (Figure 5). This feature corresponds to a repeating structure with interlayer spacing of ~ 31 Å which is identified as approximately the bilayer spacing at 1 CMC.

The Scherrer equation relates the size of a crystalline domain to the broadening of a Bragg diffraction peak[31]. This approach has been applied to determine the number of layers at an

interface by Briscoe *et al*[32]. Applied here, it is estimated that 20 to 30 bilayers are assembled at the mica/water interface at this concentration.

It is concluded that a well-ordered structure of repeating bilayers of surfactants arrange at the surface at a bulk surfactant concentration of 2 CMC: described as an $L_\alpha(c)$ phase at the interface. This is an interesting observation when the bulk solution phase is believed to be an isotropic micellar phase (L_1) and not a lamellar phase at this concentration of 1 mM. The bulk solution phase changes to an $L_1 + L_\alpha(sw)$ phase for $Ca(AOT)_2$ concentrations above 1.1 mM[33,34].

Adsorption of $Ca(AOT)_2$ at pH 4 and pH 9

The adsorption of $Ca(AOT)_2$ at the CMC at pH 4 and pH 9 was also investigated. A new mica surface for each pH was characterized in three contrasts of water: D_2O, CMSi, H_2O of the required pH. As before, the data was fitted to a three layer model for the silicon oxide, glue and mica layers. The parameters used to fit the bare surface of these crystals**,** **e**xperimental reflectivity profiles and fits to the data are given in Table 5 and Table 6.

Layer	Thickness	Roughness/ Å
Silicon Substrate	-	5.0 ± 2 Å
Silicon Oxide	25 ± 2 Å	5.0 ± 2 Å
Glue	2.6 ± 0.5 µm	7.8 ± 3 Å
Mica	14.5 ± 0.2 µm	4.5 ± 2 Å

Table 5: Parameters found from fitting of the bare surface reflectivity profiles in Figure S3 (pH 4).

Layer	Thickness	Roughness/ Å
Silicon Substrate	-	4.5 ± 2 Å
Silicon Oxide	22.0 ± 3 Å	4.5 ± 2 Å
Glue	4.3 ± 0.5µm	7.5 ± 3 Å
Mica	22.4 ± 0.2 µm	2.5 ± 2 Å

Table 6: Parameters used for fitting of the bare surface reflectivity profiles in Figure S4 at pH 9

In Figure 6 and Figure 7, a small Bragg peak can be seen at Q = 0.32 Å^{-1} and is present in the reflectivity profiles recorded at the bare mica/water interface. This feature occurs at half the Q value for the mica lattice peak of mica's monoclinic unit cell, which is two lattice layers deep[35]. This peak is usually symmetry forbidden but natural materials, such as mica, may have stacking faults or related features that make these peaks observable. This mica peak is ignored during all fitting as it should have essentially no bearing on the adsorption.

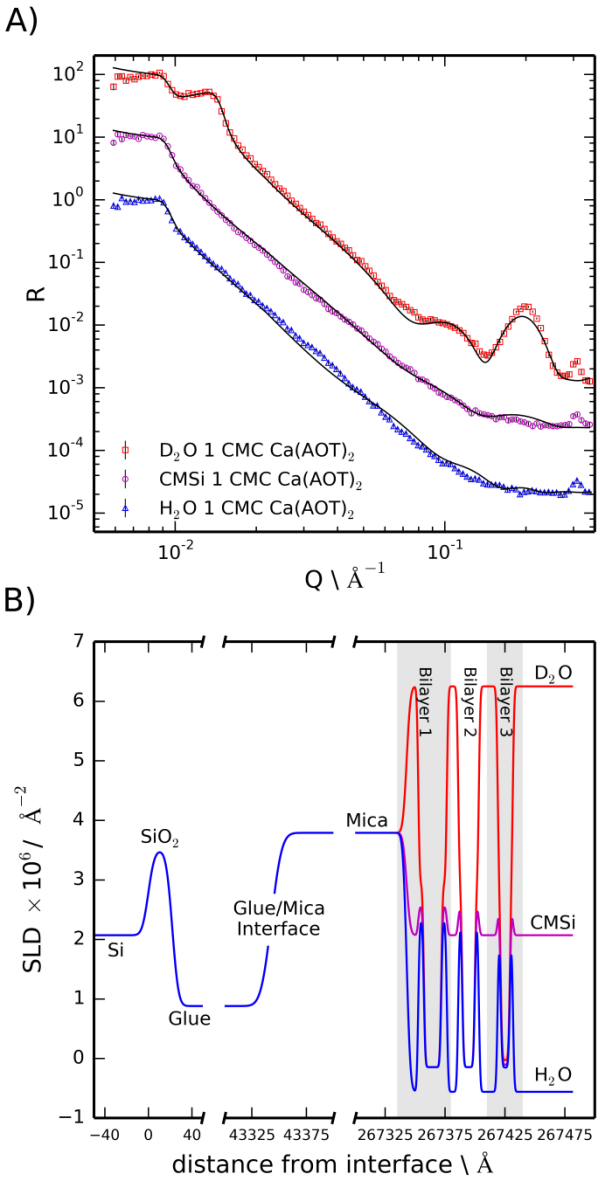

Figure 6: *A)* Observed (points) and calculated reflectivity profiles (lines) for the surface exposed to 1 CMC Ca(AOT)$_2$ at pH 9 in D_2O (squares), contrast matched to silicon water (CMSi- circles) and H_2O (triangles). Fitted lines are calculated using a three layer model for the bare surface and three stacked bilayers using the parameters given in Table 7. D_2O and H_2O data sets are offset for clarity. *B)* SLD profiles extracted from fits. The horizontal axis is split for clarity at interfaces of interest. Error bars have been included in the figure.

Layer	APM/ Å^2	Water molecules per Head	Water molecules per Tail	Roughness/ Å	Intervening Water layer thickness/ Å
1	55 ± 3	1 ± 1	0 ± 0	1 ± 1	10 ± 1
2	75 ± 4	1 ± 1	0 ± 0	1 ± 1	9 ± 1
3	101 ± 5	1 ± 1	1 ± 1	1 ± 1	16 ± 1

Table 7: Parameters used for fitting of the adsorbate structure at 1 CMC at pH 9

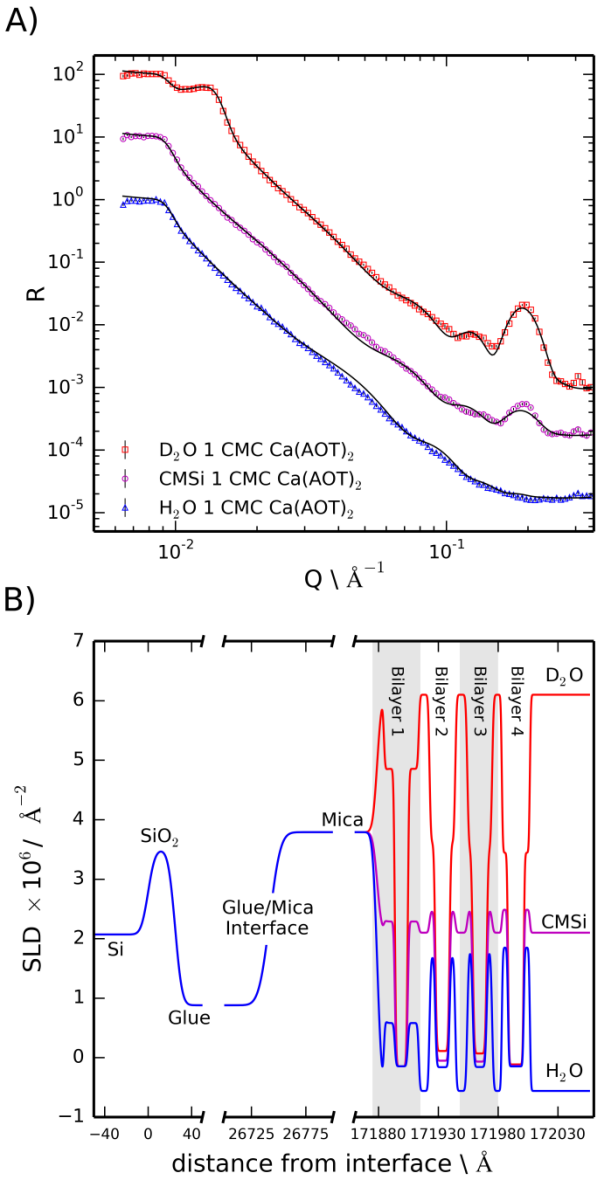

Figure 7: *A)* Observed (points) and calculated reflectivity profiles (lines) for the surface exposed to 1 CMC Ca(AOT)$_2$ at pH 4 in D_2O (squares), contrast matched to silicon water (CMSi- circles) and H_2O (triangles). Fitted lines are calculated using a three layer model for the bare surface and four stacked bilayers using the parameters given in Table 8. D_2O and H_2O data sets are offset for clarity. *B)* SLD profiles extracted from fits. The horizontal axis is split for clarity at interfaces of interest. Error bars have been included in the figure.

Bilayer	APM/ Å^2	Water molecules per Head	Water molecules per Tail	Roughness/ Å	Intervening Water layer thickness/ Å
1	80 ± 3	3 ± 1	0 ± 0	1 ± 1	10 ± 1
2	67 ± 2	9 ± 2	1 ± 1	1 ± 1	11 ± 1
3	71 ± 2	10 ± 2	0.2 ± 1	1 ± 1	5 ± 1
4	61 ± 2	3 ± 1	1 ± 1	1 ± 1	6 ± 1

Table 8: Parameters used for fitting of the adsorbate structure at 1 CMC at pH 4

The clean surfaces were exposed to 1 CMC $Ca(AOT)_2$ at pH 4 and pH 9 respectively and the reflectivity profiles recorded in D_2O, CMSi and H_2O contrasts. The data collected at pH 9 are shown in Figure 6 and the data collected at pH 4 shown in Figure 7. A large change in the reflectivity compared to the bare interface was observed for both pHs indicating that significant adsorption of the surfactant has taken place at 1 CMC for solutions at pH 4 and pH 9.

The data recorded at each pH is now discussed in detail.

pH 9

The shapes of the reflectivity profiles recorded in D_2O at pH 9 (see Figure 6) broadly show the same shapes as the corresponding profile at pH 7. The broad features occur at the same Q value at pH 7 as pH 9, indicating that the bilayer repeat spacing is essentially unaffected by a rise in the pH. As at pH 7, the data could be well fitted by a stack of three bilayers.

The best fitting model was achieved when the previous stacked bilayer model was altered to include an intervening layer of water between the surfactant headgroups of adjacent bilayers. Insufficient contrast was achieved by including the water in this region as a hydration of the headgroups. This difference between pH 7 and pH 9 experimental data indicates that a layer of water can be distinguished between bilayers at pH 9, but not at pH 7

where the more complex model reduces the goodness of fit to the data. Headgroup regions of the adsorbate must, therefore, be more disordered at pH 7 than pH 9.

The parameters used to fit the bilayers and intervening water layers are given in Table 7. We describe this structure as a S_3' adsorbed concentrated lamellar phase, $L_\alpha(c)$.

pH 4

The shape of the reflectivity profiles recorded at pH 4 differed from those recorded at pH 7 and pH 9, indicating a different adsorbate structure. A model corresponding to four stacked AOT bilayers was found to best fit the experimental data.

A model containing distinct intervening water layers between the headgroups of adjacent layers was found to provide a better fit to the data than hydrated headgroups. The model is the same as used for the S_3' structure at pH 9 for three layers, but extended to four layers. This structure is described as an S_4' multilayer adsorbate.

The fits to the data in Figure 7 are calculated according the bilayer parameters in Table 8 and the parameters determined from characterization of the bare surface given in the supplementary information.

Discussion

There are many interesting aspects to $M^{n+}(AOT)_n$ adsorption at the mica/water interface. The key phenomena have been identified and are now discussed in turn.

Cation dependency

Adsorption at the mica/water interface of the anionic surfactant AOT has been shown to be highly sensitive to the identity of the metal cation in its salt ($M^{n+}(AOT)_n$).

Divalent Ca^{2+} metal ions were shown to mediate adsorption between the like charged surface and surfactant ions at the CMC. By contrast, no adsorption occurred in the presence of Na^{+} ions. Adsorption of this anionic surfactant on the strongly negatively charged mica surface is a somewhat surprising result due to the expected electrostatic repulsion between like charged species.

Previous work studying the adsorption at the silica/water interface suggested this adsorption phenomenon happened via a cation bridging mechanism[6]. It is suggested that the multiple charge of the ion is the key property which enables $Ca(AOT)_2$ adsorption at the mica/water interface, where negative charges on both the surface and AOT anion can be simultaneously compensated by the divalent ion.

Although this work suggests that divalent ion bridging may be responsible for anion on anion adsorption, we have preliminary evidence the monovalent ion cesium also leads to adsorption of the AOT on mica. This suggests a more complicated mechanism, similar to that use to explain clay swelling, where the ion charge density is the key feature. High charge density ions (e.g. sodium) remain solvated, do not bind to the clay surface and hence form a diffuse ion cloud leading to swelling. In contrast, lower charge density ions, such as potassium and cesium, are less strongly hydrated, and are able to sacrifice bound water to bind to the clay surface and prevent swelling. Hence in clay swelling we observe analogous behavior to the cation bridging, holding two negatively charged plates together, but entirely with monovalent ions.

The adsorbed amount of $Ca(AOT)_2$ increases sharply at the CMC (only a sparse hydrated layer was observed at half CMC). Other researchers have highlighted the tendency of AOT to form lamellar structures above the CMC driven by assembly of the layers[10].

Multilayers of $Ca(AOT)_2$

Significant multilayer adsorption of the calcium salt occurs at pH 4, 7 and 9 at the CMC. 1 CMC $Ca(AOT)_2$ is adsorbed as three closely stacked bilayers (S_3') with no intervening water layers but significant hydration of the headgroups at pH 7. A S_3' structure was also measured at pH 9 but here thin water layers between the surfactant bilayers are identified. At pH 4, a S_4' structure with thin water layers was found to be consistent with the fitted data.

Adsorption of NaAOT and $Ca(AOT)_2$ salts on other mineral surfaces at the CMC (sapphire, calcite, silica) has been reported as a single bilayer[6,10,11]. The unusual S_3' and S_4' structures appear specific to the mica surface in combination with the $Ca(AOT)_2$ salt. Typically adsorbed multilayers occur when the bulk solution is in a lamellar phase and, essentially, represent a templating of the bulk phase; the experimental data presented here is an interesting case where multilayer ordering occurs at a surface where the bulk solution is still an isotropic micellar phase.

Several cases of multilayering in the presence of multivalent ions (particularly Al^{3+} and Ca^{2+}) for anionic or mixed anionic/non-ionic surfactant systems have been observed at the air/water interface[36–39]. The range of stability for a given S_n' structure was sensitive to the ion concentration, ion identity and was surfactant specific.

Multilayer adsorption in the presence of multivalet ions or polyions have been observed reasonably frequently at the air-water. Interestingly multivalent ions can also lead to multilayers at the solid/liquid interface, such as sodium dioxyethylene sulfate (SLES) and SLES / nonionic surfactant mixtures at the hydrophilic and hydrophobic silica surfaces[40]. Interestingly the extent of multilayers is reported to be enhanced by a more homogeneous surface. Hence with the mica substrate used here which should be very flat and homogeneous, we expect to see extensive multilayers.

The formation of multilayers is also related to charge reversal at surfaces by multivalent and polyion binding[40,41] One can envisage how two similarly charged surfaces can be

attracted to one another (rather than repelled) if one of the layers has the surface charged reversed by multivalent ions. Usually one requires multivalent ion so that the surface charge is over compensated. Monovalent ions may simply neutralize the surface charge. An interesting question is why such charge reversal leads to multilayers, rather than simply formation of one adsorbed bilayer, if the bulk phase is not a lamellar phase.

It is suggested that the calcium ions stabilize the formation of multilayers and that the calcium ion concentration in the salt at the CMC is "just right" to induce S_3' or S_4' multilayers on mica at the pHs studied.

Note that, no multilayering of $Ca(AOT)_2$ was seen by Wang *et al.* at the silica/water interface at the same pHs and concentrations suggesting that the mica itself also contributes to the adsorbate structure[6].

Mica contribution to adsorbate structure

Mica has a high surface charge with structural origin; one significant difference between the silica and mica surfaces. Enhanced electrostatic attraction from the surface may be involved in the multilayering on mica.

The area per AOT moiety (APM) at the inner leaflet of the first $Ca(AOT)_2$ bilayer determined for all pHs is larger than the cited area per unit charge for the mica surface (47 $Å^2$)[35]. The area per AOT moiety for either NaAOT or $Ca(AOT)_2$, in free solution or adsorbed at interfaces, has been widely measured as between 60 and 65 $Å^2$ and is not been reported below 51 $Å^2$ [6,10,11,42]. The APMs determined here for AOT are not uncharacteristic when adsorbed against the high charge mica surface, suggesting that surfactant packing constraints dominate density of the bilayer.

The behavior of the calcium ions around these layers, therefore, must play a key role in the multilayering. Two behaviors are suggested:

(1) One calcium ion remains strongly associated with one AOT anion. Adsorption can be thought of as $CaAOT^+$ adsorbing at the mica interface. In this case, the observed area per molecule indicates that the surface charge is undercompensated by the first layer.

(2) Calcium ions are not strictly paired with AOT anions so that in the region between the surface and first bilayer an enhanced concentration of calcium ions may be present. This allows for full compensation of both the surface charge and the AOT anions in the first bilayer.

In the first case, under compensation may encourage formation of additional layers to cancel the remaining surface charge not neutralized by the first bilayer, resulting in a multilayer stack. In the second case, the surface charge is fully screened by the anions and it is hard to argue on this basis why the mica surface induces multilayers and the silica surface does not.

Future work in this area will focus on pinpointing the position of the inorganic ions possibly using x-rays. Different ion behavior in the electric double layer around mica and silica surfaces appears the most likely explanation for the different structures on each surface.

pH behaviour

A similar study to this has been reported by Wang *et al.* differing only in the solid surface of interest, silica. Wang *et al.* found no adsorption of $Ca(AOT)_2$ at pH 4. In contrast, adsorption of $Ca(AOT)_2$ at pH 4 was observed for the mica/water interface. On silica, the conditions for anionic surface/anionic surfactant adsorption mediated by a divalent ion are

considered to be more favorable at higher pHs where the surface holds a higher negative charge (by dissociation of SiOH groups).

This different result is consistent with our present understanding of these systems because mica exhibits a largely pH independent structural charge from isomorphic substitution[43].

Comparing across the fitted models at pHs 4, 7 and 9 on mica, two differences are evident. First, four layers are adsorbed at pH 4 whilst only three are absorbed at pH 7 and 9. Second, thin layers of water were resolved between bilayers at pH 4 and 9, whilst at pH 7, the reflectivity was best modelled by adding hydration to the headgroup region. The origin of such variations are hard to elucidate and will probably depend on a subtle balance of electrostatics, molecule packing and water/ion hydration.

The variation in the number of adsorbed bilayer with pH is a complicated issue and there are several factors that could be relevant to this reasonably small, but significant change in the number of adsorbed layers on going from pH 7/9 to pH 4 (an increase from 3 to 4 bilayers).

Changes in the association of the head group of AOT. The pKa of AOT is rather lower than the lowest pH considered here (pH 4). Hence the degree of re-protonation is expected to increase on lowering the pH but should be rather small. If the head group is slightly less negatively charged, this might slightly reduce the inter surfactant repulsion and lead to a small increase in adsorption.

Similarly, the CMC of the AOT might be expected to change slightly on lowering the Ph (more charged surfactants can have a higher CMC due to increased repulsion between the head groups). Hence lower pH may be expected to reduce the CMC and may favour self-assembly in the bulk and at the surface. However, again we suspect this to be a very small effect over this pH range.

To alter the pH, additional acid was added which could increase the ionic strength which may screen inter head group repulsion, favouring more self-assembly at the surface. Ca(AOT)2 CMC is approx. 0.5 mM and the added acid at pH 4 corresponds to [H+] and [Cl-] of 10^{-4} M. Hence the change in pH does represent a small increase in ionic strength of about 10%.

There is often a pH variation of the surface charge of many oxide surfaces. For silica the surface is neutral at pH 2 and becomes increasingly negative charged with increasing pH. Alumina exhibits similar features but the surface is neutral at a pH around 8 and is positive below pH 8 and negative above pH 8. These changes arise from protonation/deprotonation of surface -OH groups. Interestingly mica has a surface charge that arises from isomorphic substitution of cations in the crystal lattice that can be considered to be pH independent. However, there are some Al-OH groups in the mica structure that might be involved in related speciation. Hence if there are any changes on lowering the pH, the surface of mica is expected to be less negative and more positive. This might be expected to lead to more adsorption of an ionic surfactant (AOT). However, we expect the effects to be small.

Adsorbed lamellar phase at 2 CMC

Further interesting behavior is seen on increasing the concentration of $Ca(AOT)_2$ to 2 CMC at pH 7.

At 2 CMC, $Ca(AOT)_2$ is very close to the bulk lamellar phase onset at ~1.1 mM (2.2 CMC). It appears the experimental data indicates that the mica surface is able to provide a site for early onset lamellar ordering at the surface with many layers present.

To our best knowledge, the lamellar phase spacing of $Ca(AOT)_2$ is not widely reported in the literature. Our own SANS measurements of 2% w:w $Ca(AOT)_2$ in D_2O recorded at 20°C contain a peak at 0.21 $Å^{-1}$, indicative of a 31 Å lamellar spacing in the $L_1 + L_\alpha$ bulk phase beginning at 1.1 mM. Data is shown in the supplementary information in Figure S5.

This represents significantly different behavior from NaAOT where the low concentration lamellar repeat spacing is reported in the range 170 - 220 Å[11–15]. Multivalent ions are known to promote the formation of condensed lamellar phases by promoting an additional attractive force between lamellar[44,45]. Hence, this result is not unexpected.

The adsorption of $Ca(AOT)_2$ at 2 CMC is interpreted simply as a surface providing a template for structuring of the low concentration bulk lamellar phase into a lamellar phase orientated parallel to the surface. The adsorption appears to gently perturb the bulk lamellar spacing from 31 Å to 30 Å at the surface.

Summary and conclusions

Specular neutron reflection has been applied to the study of adsorption of Aerosol-OT in the presence of metal ions with different valencies over a range of pHs. Adsorption of this anionic surfactant on the negatively charged mica surface occurs only in the presence of Ca^{2+} ions not monovalent Na^{+}. An unusual multilayer ordering of $Ca(AOT)_2$ is observed at the mica/water interface.

Significant adsorption occurs at and above the bulk solution CMC. The adsorbate structure was fitted to three closely stacked bilayers with no intervening water between adjacent bilayers at pH 7 (S_3), four bilayers with a thin intervening water layer (S_4) at pH 4 and three bilayers with a thin intervening water layer (S_3) at pH 9.

Adsorption of collapsed lamellar of surfactant molecules is thought to result from the ability of calcium to shield electrostatic interactions between adjacent lamellar and act as a link between the mica surface and the anionic surfactant chains. This is not possible for the monovalent salt Na^{+} leading to no adsorption as shown in this study; thus accounting for the ion specificity of the adsorption.

It is suggested that in the absence of a pH dependent surface charge, variations with pH originate from electrostatic screening of headgroups as H^+ and OH^- ions contribute as a background electrolyte.

Details of both the surface and solution behavior seem important in the adsorption of this surfactant at the mica/water interface.

Supporting information

Bare surface reflectivity profiles and fitted parameters for the bare surfaces of pH 4 and pH 9 mica crystals.

Additional figure displaying reflectivity data recorded at the mica/water interface exposed to 0.1 CMC, 0.25 CMC and 0.5 CMC $Ca(AOT)_2$ in D_2O.

This material is available free of charge via the Internet at http://pubs.acs.org.

Author Information

Please address correspondence to:

Stuart Clarke (stuart@bpi.cam.ac.uk)

Acknowledgements

We would like to thank the beam time committee for awarding the time to undertake this study at ISIS (RB1410157). Further thanks are extended to Andy Pluck (BP Institute), Andy Church (ISIS Sample environment), Alasdair Ross and Sean Peacock (University of

Cambridge Engineering Department) for help manufacturing and designing sample cells. Finally, we thank BP for funding the work and our industrial colleagues, Isabella Stocker and Peter Salino, for their scientific contributions to the work (RG63491).

References

(1) Thomas, R. K.; Penfold, J. Multilayering of Surfactant Systems at the Air-Dilute Aqueous Solution Interface. *Langmuir* **2015**, *31*, 7440–7456.

(2) Li, Z. X.; Lu, J. R.; Thomas, R. K.; Penfold, J. Neutron Reflectivity Studies of the Adsorption of Aerosol-OT at the Air - Water Interface : The Structure of the Sodium Salt. **1997**, *5647*, 1615–1620.

(3) Mukerjee, P.; Mysels, K. J. Critical Micelle Concentrations of Aqueous Surfactant Systems. *National Standards Reference Data Systems*, 1971, 1–222.

(4) Rogers, J.; Winsor, P. A. Change in the Optic Sign of the Lamellar Phase (G) in the Aerosol OT/water System with Composition or Temperature. *J. Colloid Interface Sci.* **1969**, *30*, 247–257.

(5) Eastoe, J.; Fragneto, G.; Robinson, B. H.; Towey, T. F.; Heenan, R. K.; Leng, F. J. Variation of Surfactant Counterion and Its Effect on the Structure and Properties of Aerosol-OT-Based Water-in-Oil Microemulsions. *J. Chem. Soc. Faraday Trans.* **1992**, *88*, 461–471.

(6) Wang, X.; Lee, S. Y.; Miller, K.; Welbourn, R.; Stocker, I.; Clarke, S.; Casford, M.; Gutfreund, P.; Skoda, M. W. A. Cation Bridging Studied by Specular Neutron Reflection. *Langmuir* **2013**, *29*, 5520–5527.

(7) Zapf, A.; Beck, R.; Platz, G.; Hoffmann, H. *Calcium Surfactants: A Review*; 2003; Vol. 100–102.

(8) Khan, A. Phase Equilibria in the Mixed Sodium and Calcium Di-2-Ethylhexylsulfosuccinate Aqueous System. An Illustration of Repulsive and Attractive Double-Layer Forces. *J Phys. Chem.* **1985**, *89*, 5180–5184.

(9) Fragneto, G.; Li, Z. X.; Thomas, R. K.; Rennie, A. R.; Penfold, J. A Neutron Reflectivity Study of the Adsorption of Aerosol-OT on Self-Assembled Monolayers on Silicon. *J. Colloid Interface Sci.* **1996**, *178*, 531–537.

(10) Hellsing, M. S.; Rennie, A. R.; Hughes, A. V. Effect of Concentration and Addition of Ions on the Adsorption of Aerosol-OT to Sapphire. *Langmuir* **2010**, *26*, 14567–14573.

(11) Stocker, I. N.; Miller, K. L.; Welbourn, R. J. L.; Clarke, S. M.; Collins, I. R.; Kinane, C.; Gutfreund, P. Adsorption of Aerosol-OT at the Calcite/water Interface--Comparison of the Sodium and Calcium Salts. *J. Colloid Interface Sci.* **2014**, *418*, 140–146.

(12) Li, Z. X.; Weller, A.; Thomas, R. K.; Rennie, A. R. Adsorption of the Lamellar Phase of Aerosol-OT at the Solid / Liquid and Air / Liquid Interfaces. *J Phys Chem B* **1999**, *103*, 10800–10806.

(13) Hellsing, M. S.; Rennie, A. R. Adsorption of Aerosol-OT to Sapphire : Lamellar Structures Studied with Neutrons. *Langmuir* **2011**, *27*, 4669–4678.

(14) Li, Z. X.; Lu, J. R.; Thomas, R. K.; Weller, A.; Penfold, J.; Webster, J. R. P.; Sivia, D. S.; Rennie, A. R. Conformal Roughness in the Adsorbed Lamellar Phase of Aerosol-OT at the Air - Water and Liquid - Solid Interfaces. *Langmuir* **2001**, *17*, 5858–5864.

(15) Li, X. X.; Thomas, R. K.; Lu, J. ren; Penfold, J. Neutron Specular and off-Specular Reflection from the Surface of Aerosol-OT Solutions above the Critical Micelle Concentration. *Faraday Discuss.* **1996**, *104*, 127–138.

(16) Browning, K. L.; Griffin, L. R.; Gutfreund, P.; Barker, R. D.; Clifton, L. A.; Hughes, A.; Clarke, S. M. Specular Neutron Reflection at the Mica Water Interface. *J. Appl. Crystallogr.* **2014**, *47*, 1638–1646.

(17) Briscoe, W. H.; Chen, M.; Dunlop, I. E.; Klein, J.; Penfold, J.; Jacobs, R. M. J. Applying Grazing Incidence X-Ray Reflectometry (XRR) to Characterising Nanofilms on Mica. *J. Colloid Interface Sci.* **2007**, *306*, 459–463.

(18) Briscoe, W. H.; Speranza, F.; Li, P.; Konovalov, O.; Bouchenoire, L.; van Stam, J.; Klein, J.; Jacobs, R. M. J.; Thomas, R. K. Synchrotron XRR Study of Soft Nanofilms at the Mica–Water Interface. *Soft Matter* **2012**, *8*, 5055–5068.

(19) Speranza, F.; Pilkington, G. A.; Dane, T. G.; Cresswell, P. T.; Li, P.; Jacobs, R. M. J.; Arnold, T.; Bouchenoire, L.; Thomas, R. K.; Briscoe, W. H. Quiescent Bilayers at the Mica–Water Interface. *Soft Matter* **2013**, *9*, 7028–7041.

(20) Griffin, L. R.; Browning, K. L.; Truscott, C. L.; Clifton, L. A.; Clarke, S. M. Complete Bilayer Adsorption of C16TAB on the Surface of Mica Using Neutron Reflection. *J. Phys. Chem. B* **2015**, *119*, 6457−6461.

(21) Griffin, L. R.; Browning, K. L.; Truscott, C. L.; Clifton, L. A.; Webster, J.; Clarke, S. M. A Comparison of Didodecyldimethylammonium Bromide Adsorbed at Mica/water and Silica/water Interfaces Using Neutron Reflection. *J. Colloid Interface Sci.* **2016**, *478*, 365–373.

(22) Eastoe, J.; Young, W. K.; Robinson, B. H.; Steytler, D. C. Scattering Studies of

Microemulsions in Low-Density Alkanes. *J. Chem. Soc. Faraday Trans.* **1990**, *86*, 2883.

(23) http://www.isis.stfc.ac.uk.

(24) Webster, J.; Holt, S.; Dalgliesh, R. INTER the Chemical Interfaces Reflectometer on Target Station 2 at ISIS. *Phys. B Condens. Matter* **2006**, *385–386*, 1164–1166.

(25) Heenan, R. K.; Rogers, S. E.; Turner, D.; Terry, A. E.; Treadgold, J.; King, S. M. Small Angle Neutron Scattering Using Sans2d. *Neutron News* **2011**, *22*, 19–21.

(26) http://www.mantidproject.org.

(27) Wignall, G. D.; Bates, F. S. Absolute Calibration of Small Angle Neutron Scattering Data. *J. Appl. Crystallogr.* **1987**, *20*, 28–40.

(28) Heavens, O. S. *Optical Properties of Thin Solid Films*; Dover Publications, 1955.

(29) Zarbakhsh, A.; Querol, A.; Bowers, J.; Webster, J. R. P. Structural Studies of Amphiphiles Adsorbed at Liquid-Liquid Interfaces Using Neutron Reflectometry. *Faraday Discuss.* **2005**, *129*, 155–167.

(30) Eastoe, J.; Towey, T.; Robinson, B. H.; Williams, J.; Heenan, R. K. Structures of Metal Bis (2-Ethylhexylsulfosuccinate) Aggregates in Cyclohexane. *J. Phys. Chem.* **1993**, *97*, 1459–1463.

(31) Patterson, A. L. The Scherrer Formula for X-Ray Particle Size Determination. *Phys. Rev.* **1939**, *56*, 978–982.

(32) Dane, T. G.; Cresswell, P. T.; Bikondoa, O.; Newby, G. E.; Arnold, T.; Faul, C. F. J.; Briscoe, W. H. Structured Oligo(aniline) Nanofilms via Ionic Self-Assembly. *Soft Matter* **2012**, *8*, 2824–2832.

(33) Khan, A.; Fontell, K.; Lindman, B. Phase Equilibria of Some Ionic Surfactant Systems with Divalent Counter-Ions. *Colloids and surfaces* **1984**, *11*, 401–408.

(34) Khan, A.; Fontell, K.; Lindman, B. Liquid Crystallinity in Systems of Magnesium and Calcium Surfactants: Phase Diagrams and Phase Structures in Binary Aqueous Systems of Magnesium and. *J. Colloid Interface Sci.* **1984**, *101*, 193–200.

(35) Van Olphen, H. *Introduction to Clay Colloid Chemistry*; Wiley, 1977.

(36) Xu, H.; Thomas, R. K.; Petkov, J. T.; Tucker, I.; Webster, J. P. R. The Formation of Surface Multilayers at the Air − Water Interface from Sodium Diethylene Glycol Monoalkyl Ether Sulfate/AlCl 3 Solutions: The Role of the Alkyl Chain Length. *Langmuir* **2013**, *29*, 12744–12753.

(37) Xu, H.; Penfold, J.; Thomas, R. K.; Petkov, J. T.; Tucker, I.; Webster, J. P. R. The Formation of Surface Multilayers at the Air−Water Interface from Sodium Polyethylene Glycol Monoalkyl Ether Sulfate/AlCl3 Solutions: The Role of the Size of the Polyethylene Oxide Group. *Langmuir* **2013**, *29*, 11656–11666.

(38) Petkov, J. T.; Tucker, I. M.; Penfold, J.; Thomas, R. K.; Petsev, D. N.; Dong, C. C.; Golding, S.; Grillo, I. The Impact of Multivalent Counterions, Al3+, on the Surface Adsorption and Self-Assembly of the Anionic Surfactant Alkyloxyethylene Sulfate and Anionic/nonionic Surfactant Mixtures. *Langmuir* **2010**, *26*, 16699–16709.

(39) Penfold, J.; Thomas, R. K.; Dong, C. C.; Tucker, I.; Metcalfe, K.; Golding, S.; Grillo, I. Equilibrium Surface Adsorption Behavior in Complex Anionic/nonionic Surfactant Mixtures. *Langmuir* **2007**, *23*, 10140–10149.

(40) Penfold, J.; Thomas, R. K.; Li, P.; Xu, H.; Tucker, I. M.; Petkov, J. T.; Sivia, D. S. Multivalent-Counterion-Induced Surfactant Multilayer Formation at Hydrophobic and

Hydrophilic Solid–Solution Interfaces. *Langmuir* **2015**, *31*, 6773–6781.

(41) Penfold, J.; I. Tucker; Staples, E.; Thomas, R. K. Manipulation of the Adsorption of Ionic Surfactants onto Hydrophilic Silica Using Polyelectrolytes. *Langmuir* **2004**, *20*, 7177–7182.

(42) Fontell, K. The Structure of the Lamellar Liquid Crystalline Phase in Aerosol OT-Water System. *J. Colloid Interface Sci.* **1973**, *44*, 318–329.

(43) van Olphen, H. *Introduction to Clay Colloidal Chemistry*; 2nd ed.; Wiley, 1977.

(44) Guldbrand, L.; Jönsson, B.; Wennerström, H.; Linse, P. Electrical Double Layer Forces. A Monte Carlo Study. *J. Chem. Phys.* **1984**, *80*, 2221–2228.

(45) Khan, A.; Lindman, B.; Wennerstrom, H.; Zapf. Ionic Surfactants with Divalent Electrostatic Effects . Divalent Contra Monovalent. *Adv. Colloid Interface Sci.* **1991**, *34*, 433–449.

Graphical abstract